INTEGRATED APPROACH TO TEXTURE SEGMENTATION USING MULTIPLE GABOR FILTERS

Thomas P. Weldon

University of North Carolina
Department of Electrical Engineering
Charlotte, NC, USA 28223
E-mail: tpweldon@uncc.edu

William E. Higgins

Penn State University
Department of Electrical Engineering
University Park, PA, USA 16802
E-mail: weh@ruth.ece.psu.edu

ABSTRACT

This paper presents an integrated approach using multiple Gabor filters for the segmentation of multi-textured images. The approach includes both the design of the constituent Gabor filters and the design of the classifier and postprocessing. The classifier uses a mixture density to reduce localization error at texture boundaries, and the postprocessing uses morphological operators to remove spurious misclassifications at texture boundaries. Results are presented that confirm the efficacy of the postprocessing methods and the overall integrated approach.

1. INTRODUCTION

[1] The segmentation of textured images remains a difficult problem in image processing [1–5]. Earlier Gabor filter-based texture-segmentation methods employed: (1) a *filter-bank*, made up of a large bank of *ad hoc* selected Gabor filters with predetermined parameters; or (2) a *filter-design* approach, where a small set of Gabor filters is specifically designed to solve a particular problem [6–10]. The large number of filters used in filter-bank approaches can lead to associated disadvantages in computing a large number of filtered images and classifying a large-dimension feature space [1–3, 11]. Early efforts with the filter-design approach handled few textures (typically 2) or focused on $1-2$ filters only [9, 10].

Our work addresses the filter-design approach. Recently, we proposed a new method for the design of multiple Gabor filters for segmenting multi-textured (≥ 2) images [12, 13]. The new method provides an integrated approach that generates both the filter designs and necessary postprocessing for a complete texture-segmentation system. This method removes restrictions on the number of filters and on the number of textures. The new method offers the potential to handle more complex texture-segmentation problems without using an inordinate numbr of *ad hoc* filters.

As part of our research, we are interested in texture segmentation with a small number of Gabor filters. Not unexpectedly, experimental evidence suggests that segmentation error tends to increase as the number of filters decrease, particularly near texture boundaries. This increase in error largely appears to be driven both by the contradictory demands of low classification error and high spatial resolution and by complex relationships between feature-vector dimensionality and multidimensional decision surfaces. To address these potential sources of error, we propose a classifier that is based on a mixture density to reduce localization error at texture boundaries, and we propose morphological postprocessing to remove spurious misclassifications at texture boundaries. The remainder of this paper describes our methods, outlines the classifier and postprocessing scheme, and provides some representative results.

2. MULTICHANNEL SCHEME

Fig. 1 illustrates the general k-channel texture-segmentation scheme that we use. The input image $i(x, y)$ is assumed to be composed of $\mathcal{N}$ disjoint textures $t_1, t_2, \ldots, t_{\mathcal{N}}$ with $\mathcal{N} \geq 2$. A single *filter channel* in the scheme consists of a bandpass Gabor *prefilter* $h_j(x, y)$, a magnitude operator, and a Gaussian *postfilter* $g_{p_j}(x, y)$. References [5, 6, 8, 9] justify the components making up each filter channel.

The *Gabor prefilter* has impulse response $h_j(x, y)$, where the subscript j denotes the particular filter channel and $1 \leq j \leq k$:

$$h_j(x,y) \quad = \quad \frac{1}{2\pi\sigma_{g_j}^2}\, e^{-\frac{(x^2+y^2)}{2\sigma_{g_j}^2}} \quad e^{-j2\pi(u_j x + v_j y)} \,. \quad (1)$$

The function $h_j(x, y)$ is a complex sinusoid centered at frequency (u_j, v_j) modulated by a Gaussian envelope of spatial extent σ_{g_j} [10]. For simplicity, we also assume that the Gaussian envelope of $h_j(x, y)$ is a symmetric function. Next, the output of a prefilter stage $i_{h_j}(x, y)$ is the convolution of the input image with the Gabor prefilter

$$i_{h_j}(x,y) = h_j(x,y) * \; i(x,y) \quad (2)$$

where $*$ denotes convolution in two dimensions, and the subscript h_j indicates the output of the Gabor prefilter in the j^{th} filter channel. The magnitude of the Gabor-prefilter output is computed in the following stage as

$$m_j(x,y) = |i_{h_j}(x,y)| = |\; h_j(x,y) * \; i(x,y) \;| \quad (3)$$

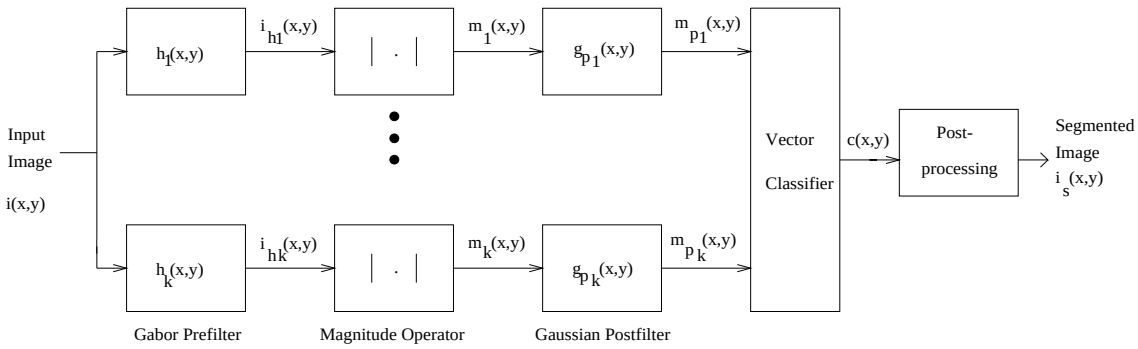

Figure 1: Multichannel scheme for segmenting a textured image.

where $m_j(x,y)$ has been shown to have approximately Rician statistics for filtered textures [6–8,13]. A lowpass *Gaussian postfilter* $g_{p_j}(x,y)$ is then applied to $m_j(x,y)$ yielding the postfiltered image in the j^{th} filter channel

$$m_{p_j}(x,y) \quad = \quad m_j(x,y) * \; g_{p_j}(x,y) \tag{4}$$

with

$$g_{p_j}(x,y) \quad = \quad \frac{1}{2\pi\sigma_{p_j}^2} \; e^{-\frac{(x^2+y^2)}{2\sigma_{p_j}^2}} \tag{5}$$

where σ_{p_j} determines the Gaussian postfilter in the j^{th} channel. Thus, the parameters $(u_j, v_j, \sigma_{g_j}, \sigma_{p_j})$ completely determine filter channel j. Moreover, the values of the filter parameters are free to vary from channel to channel. Generally, we will refer to $i_{h_j}(x,y)$ as the *prefiltered image*, $m_j(x,y)$ as the *prefilter output*, and $m_{p_j}(x,y)$ as the *postfilter output* for the j^{th} channel.

A vector classifier generates the classified image $c(x,y)$ based on the vector output of the k filter channels. A Bayesian classifier based on predicted multivariate output statistics is used. Finally, provision is made for morphological postprocessing to address misclassifications at boundaries between different textures. The result of the additional postprocessing of the classified image $c(x,y)$ gives the final segmented image $i_s(x,y)$.

3. CLASSIFIER AND POSTPROCESSING

Below, we give more detail on the proposed classifier and morphological postprocessing for the multichannel scheme of Fig. 1. First, we describe the use of a mixture density in the classifier to reduce localization error in the vicinity of texture boundaries. Then, we discuss the use of a hybrid "n-ary" morphological operation to remove spurious misclassifications near texture boundaries. The following discussion assumes that the filter channels have been designed using the methods in [12, 13].

3.1. Mixture Density Classifier

In previous research on the design of single filter channels, we presented a Gaussian statistical model for the postfiltered output $m_{p_j}(x,y)$ [6–8]. The success of this statistical model in predicting single-channel texture segmentation error and in developing single-channel design algorithms leads us to consider a multivariate Gaussian model for the vector output statistics of a set of k filter channels.

Following the single-channel development of [7, 8, 13], the envelope $m_j(x,y)$ of the prefiltered image in the j^{th} filter channel has an approximately Rician distribution. The postfiltering operation in the filter channel performs a spatial average of the prefilter output $m_j(x,y)$, leading to an approximately Gaussian distribution for the postfilter output $m_{p_j}(x,y)$. The multivariate Gaussian pdf of the filter-channel output for input texture t_i is then

$$p_i(\boldsymbol{m_p}, \boldsymbol{C_i}\,) = \tag{6}$$

$$\frac{1}{(2\pi)^{k/2}|\boldsymbol{C_i}\;|^{1/2}} \quad e^{-(\frac{(\boldsymbol{m_p}-\boldsymbol{\mu_i})^T \boldsymbol{C_i}^{-1}(\boldsymbol{m_p}-\boldsymbol{\mu_i})}{2})},$$

where $\boldsymbol{m_p} = [m_{p_1}\; m_{p_2} \ldots\; m_{p_k}]^T$ is a vector sample of the k-dimensional postfilter-output vector, $\boldsymbol{C_i}$ is the covariance matrix of the postfilter outputs, and $\boldsymbol{\mu_i} = [\mu_{i_1}\; \mu_{i_2} \ldots\; \mu_{i_k}]^T = E[\boldsymbol{m_p}]$ is the mean postfilter-output vector.

The components μ_{ij} of mean vector $\boldsymbol{\mu_i}$ can be determined for each texture t_i and each filter channel j using the single-filter methods of [7,8]. The covariance matrix $\boldsymbol{C_i}$ presents greater difficulty, since it implies a need for samples of the postfilter output for all candidate filters. However, the single-filter methods of [7, 8] do yield the diagonal elements of the covariance matrix, and these correspond to the variances $s_{p_{ij}}^2$ of the output of individual filter channels. Thus, we propose using the values of $s_{p_{ij}}^2$ along the diagonal of $\boldsymbol{C_i}$ with all off-diagonal elements equal to zero. To reduce the likelihood of having strongly correlated features, the candidate filters are restricted such that the spatial-frequency responses of any of the constituent filters do not overlap significantly [13].

In practice, we have seen that a Bayesian vector classifier based on the pdf's in (6) performs well within textured regions but can exhibit *localization error* at texture boundaries; i.e., the boundary is displaced from its true location [13]. We also have observed that this localization error at texture boundaries is reduced by modifying the Bayesian classifier using a mixture density. This mixture-density approach has the advantage that it is readily implemented

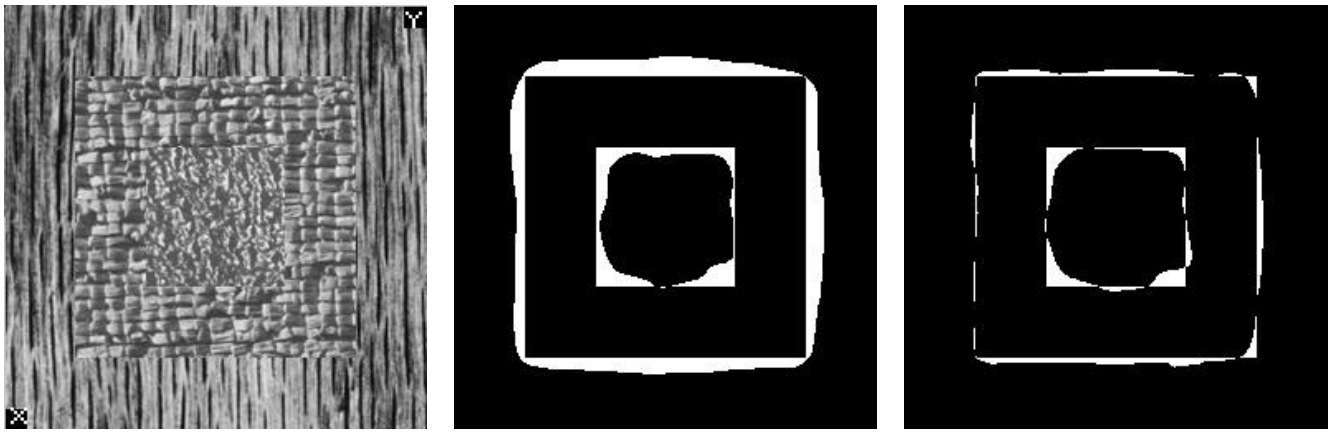

(a) (b) (c)

Figure 2: Reduction of localization error using mixture density. (a) Input composite image, outer border = d68 "wood grain," middle ring = d84 "raffia," center square = d24 "pressed leather." (b) Segmentation error without using mixture density, measured segmentation error = 0.10, misclassified pixels in white. (c) Segmentation error using mixture density, measured segmentation error = 0.04, misclassified pixels in white. Only three filter channels were used for the segmentations in (b) and (c) with parameters $(u_j, v_j, \sigma_{g_j}, \sigma_{p_j})$ = (0.14,0,6,9.6), (-0.22,0.28,3,4.8), and (0.27,0.02,3,4.8).

for the present case of multivariate-Gaussian classes. The procedure for generating the classifier is to first select the largest variances $s^2_{p_{max_j}}$ along each feature axis corresponding to each filter channel j:

$$s^2_{p_{max_j}} \geq s^2_{p_{\alpha j}}, \qquad \alpha \in \{1, 2, \ldots \mathcal{N}\} \tag{7}$$

Then, form a covariance matrix $\boldsymbol{C_{max}}$, whose diagonal elements are the maximum variances $s^2_{p_{max_j}}, j = 1, 2, \ldots k$. For texture t_i, the multivariate form of the mixture density p_{mix_i} is then

$$p_{mix_i}(\boldsymbol{m_p}) = \frac{1}{2}\Big(p_i(\boldsymbol{m_p}, \boldsymbol{C_{max}}) + p_i(\boldsymbol{m_p}, \boldsymbol{C_i})\Big), \tag{8}$$

where $p_i(\boldsymbol{m_p}, \boldsymbol{C_i})$ is the original multivariate Gaussian pdf from (6) and $p_i(\boldsymbol{m_p}, \boldsymbol{C_{max}})$ is the multivariate Gaussian formed by taking the maximum diagonal elements of all the covariance matrices for the textures. The proposed classifier for texture segmentation is then a Bayesian classifier assigning the output to the texture whose mixture density has the largest probability density; i.e. $c(x, y) = \alpha$ such that

$$p_{mix_\alpha}(\boldsymbol{m_p}(x, y)) \geq p_{mix_\beta}(\boldsymbol{m_p}(x, y)), \qquad \forall\, \beta \tag{9}$$

where $\beta \in \{1, 2, \ldots, \mathcal{N}\}$, and p_{mix_β} is the mixture density for texture t_β given in (8).

3.2. Morphological Postprocessing

Another difficulty observed in practice is the appearance of narrow regions in $c(x, y)$ that are misclassified as a third texture near the boundary between two textures. These narrow misclassified regions appear to be caused by the trajectory of the feature vector as it makes the transition through feature space at the boundary. A two-step hybrid "n-ary" morphological postprocessing operation is used to reduce these narrow misclassified regions. In the first step, pixels in $c(x, y)$ whose neighborhood (neighborhood size proportional to spatial extent of filter-channel response) consists entirely of one texture class are left unchanged; otherwise, the pixel value is set to zero to indicate it is no longer assigned to any class. This first step resembles a morphological erosion operation. In the second step, the classified regions are propagated back into the unassigned regions based on the most common class within 8-neighborhoods. This second step resembles a morphological dilation operation. The resultant image is then the final segmented image $i_s(x, y)$.

Alternative classifier and postprocessing approaches are the topic of ongoing research [13]. However, the present methods serve to illustrate the effectiveness of the designed filters in a complete system while addressing issues that can arise when a small number of filter channels is used relative to the number of textures [12, 13].

4. RESULTS

Experimental results that illustrate the complete system of Fig. 1 with a particular focus on the effects of the mixture-density classifier are shown in Fig. 2. The image in Fig. 2(a) consists of three Brodatz textures: an outermost region of "d68 - wood grain", a middle ring of "d84 - raffia", and an innermost square region of "d24 - pressed leather" [14]. Fig. 2(b) shows the segmentation error (misclassified pixels are the white regions) in $i_s(x, y)$ when the mixture density is *not* used; i.e., with Bayesian classification based on (6). Fig. 2(c) shows the segmentation error when the mixture density of (8) is used for classification. Morphological postprocessing was not altered in Figs. 2(b) and (c), so that only the effect of modifying the classifier is observed. The improvement near texture boundaries that is apparent in comparing Figs. 2(b) and (c) is confirmed by the reduction of total measured error from 10% to 4%.

The results in Fig. 3 illustrate the effects of the mor-

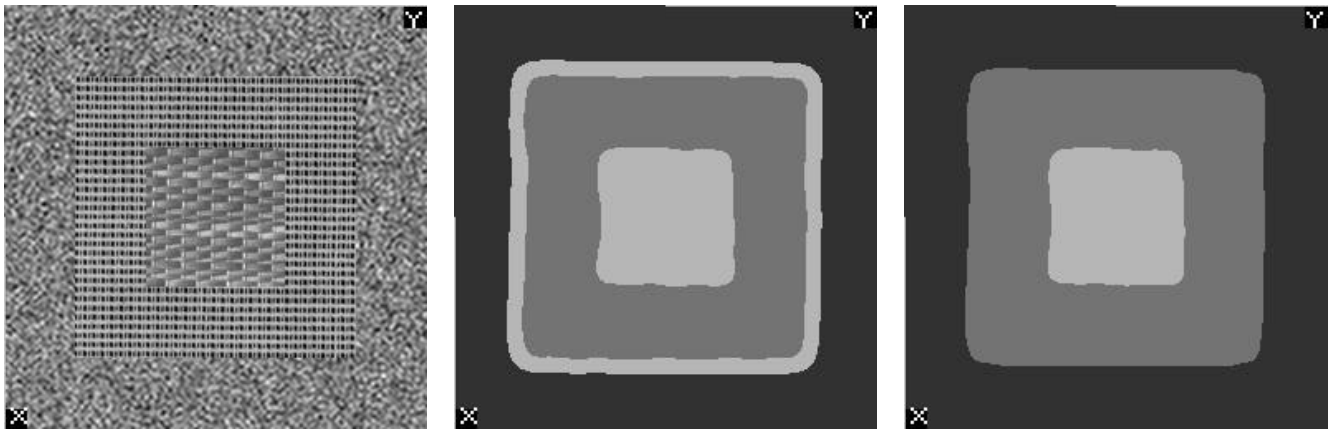

(a) (b) (c)

Figure 3: Reduction of missclassifications near texture-boundaries using morphological postprocessing. (a) Input composite image, outer border = lowpass noise, middle ring = d21 "french canvas," center square = d55 "straw matting." (b) Output of mixture-density classifier $c(x, y)$ showing pronounced misclassification error at boundary between the outermost region of lowpass noise texture and the middle region of d21 texture. Note that the boundary is misclassified as the third (innermost) texture, d55. (c) Final segmentation after morphological postprocessing to remove localization error at texture boundaries, measured segmentation error = 0.05. Only two filter channels were used for the results in (b) and (c) with parameters $(u_j, v_j, \sigma_{g_j}, \sigma_{p_j})$ = (0,0.36,3,4.8) and (-0.17,0.41,3,4.8).

phological postprocessing on misclassifications at texture boundaries. The image in Fig. 3(a) consists of an outermost region of lowpass noise, a middle ring of "d21 - french canvas", and an innermost square region of "d55 - straw matting". Fig. 3(b) is the classifier output $c(x, y)$ using a mixture-density. A prominent band of misclassified pixels is seen along the entire boundary between the outermost texture (lowpass noise) and the middle ring of texture (d21). The misclassification appears to be caused by the trajectory of the feature-vector as it makes the transition between the two textures. During the transition between the two outermost textures, the vector appears to travel through a region in feature space that is assigned to the third texture (the texture at the center of the image). Finally, morphological postprocessing is applied to Fig. 3(b), resulting in the final segmented image $i_s(x, y)$ shown in Fig. 3(c). The mixture-density classifier was not altered in Figs. 3(b) and (c), so that only the effect of adding morphological postprocessing is observed. Comparing Fig. 3(b) and (c), the misclassified pixels at the texture boundary are mitigated by morphological postprocessing.

5. REFERENCES

[1] A. K. Jain and F. Farrokhnia, "Unsupervised texture segmentation using Gabor filters," *Pattern Recognition*, vol. 23, no. 12, pp. 1167–1186, Dec. 1991.

[2] T. Randen and J. H. Husøy, "Multichannel filtering for image texture segmentation," *Optical Eng.*, vol. 33, no. 8, pp. 2617–2625, Aug. 1994.

[3] T. Chang and C. C. J. Kuo, "Texture analysis and classification with tree-structured wavelet transform," *IEEE Trans. Image Proc.*, vol. 2, no. 4, pp. 429–441, Oct. 1993.

[4] J. G. Daugman, "Uncertainty relation for resolution in space, spatial frequency, and orientation optimized by two-dimensional visual cortical filters," *J. Opt. Soc. Amer. A*, vol. 2, no. 7, pp. 1160–1169, July 1985.

[5] D. Dunn, W. Higgins, and J. Wakeley, "Texture segmentation using 2-D Gabor elementary functions," *IEEE Trans. Pattern Anal. Machine Intell.*, vol. 16, no. 2, pp. 130–149, Feb. 1994.

[6] T. P. Weldon, W. E. Higgins, and D. F. Dunn, "Efficient Gabor filter design for texture segmentation," *Pattern Recognition*, vol. 29, no. 12, pp. 2005–2015, Dec. 1996.

[7] T. P. Weldon and W. E. Higgins, "Multiscale Rician approach to Gabor filter design for texture segmentation," in *IEEE Int. Conf. on Image Processing*, vol. II, (Austin, TX), pp. 620–624, 13-16 Nov. 1994.

[8] T. P. Weldon, W. E. Higgins, and D. F. Dunn, "Gabor filter design for multiple texture segmentation," *Optical Eng.*, vol. 35, no. 10, pp. 2852–2863, Oct. 1996.

[9] A. C. Bovik, "Analysis of multichannel narrow-band filters for image texture segmentation," *IEEE Trans. Signal Processing*, vol. 39, no. 9, pp. 2025–2043, Sept. 1991.

[10] D. F. Dunn and W. E. Higgins, "Optimal Gabor filters for texture segmentation," *IEEE Trans. Image Proc.*, vol. 4, no. 7, pp. 947–964, July 1995.

[11] R. O. Duda and P. E. Hart, *Pattern Classification and Scene Analysis*. John Wiley and Sons, 1973.

[12] T. Weldon and W. Higgins, "Design of multiple Gabor filters for texture segmentation," in *Proc. IEEE Int. Conf. Acoust., Speech, Signal Processing* , vol. IV, (Atlanta, GA), pp. 2245–2248, 7-10 May 1996.

[13] T. P. Weldon, *Multiresolution Design of Multiple Gabor Filters for Texture Segmentation*. PhD thesis, The Pennsylvania State University, 1995.

[14] P. Brodatz, *Textures: A Photographic Album for Artists and Designers*. New York, NY: Dover, 1966.

[15] I. Bloch, "Fuzzy connectivity and mathematical morphology," *Pattern Recog. Lett.*, vol. 14, no. 6, p. 483, June 1993.